

# Valley-selective Floquet Chern Flat Bands in Twisted Multilayer Graphene

Ming Lu,<sup>1,2</sup> Jiang Zeng,<sup>2</sup> Haiwen Liu,<sup>3</sup> Jin-Hua Gao,<sup>4,\*</sup> and X. C. Xie<sup>2,1,5,†</sup>

<sup>1</sup>Beijing Academy of Quantum Information Sciences, Beijing 100193, China

<sup>2</sup>International Center for Quantum Materials, School of Physics, Peking University, Beijing 100871, China

<sup>3</sup>Center for Advanced Quantum Studies, Department of Physics,  
Beijing Normal University, Beijing 100875, China

<sup>4</sup>School of Physics and Wuhan National High Magnetic Field Center,  
Huazhong University of Science and Technology, Wuhan 430074, China

<sup>5</sup>CAS Center for Excellence in Topological Quantum Computation,  
University of Chinese Academy of Sciences, Beijing 100190, China

(Dated: July 31, 2020)

We show that Floquet engineering with circularly polarized light (CPL) can selectively split the valley degeneracy of a twisted multilayer graphene (TMG), and thus generate a controlled valley-polarized Floquet Chern flat band with tunable large Chern number. It offers a feasible optical way to manipulate the valley degree of freedom in moiré flat bands, and hence opens new opportunities to study the valleytronics of moiré flat band systems. We thus expect that many of the valley-related properties of TMG, *e.g.* orbital ferromagnetism, can be switched by CPL with proper doping. We reveal a Chern number hierarchy rule for the Floquet flat bands in a generic (M+N)-layer TMG. We also illustrate that the CPL effects on TMG strongly rely on the stacking chirality, which is an unique feature of TMG. All these phenomena could be tested in the twisted double bilayer graphene systems, which is the simplest example of TMG and has already been realized in experiment.

*Introduction.*— The topological flat bands in twisted multilayer graphene (TMG) have drawn great research interest very recently, because that a Chern flat band is believed to be a promising platform to realize fractional Chern insulator and may harbour novel correlation states [1–26]. The most generic situation is a (M+N)-layer TMG, where two ABC-stacked multilayer graphene (MG) are stacked on top of each other with a small twist angle [8]. Twisted double bilayer graphene (TDBG) is the simplest example, *i.e.*, the case of  $M = 2$ ,  $N = 2$ , and has already been realized in experiment [1–4]. In TMG, a pair of flat bands are formed around the magic angle, which locate at two inequivalent valleys in momentum space. The two flat bands can be isolated by a vertical electric field and have nonzero valley Chern numbers [5–10]. The topological flat band is an unique feature of TMG. Another special characteristic of TMG is that it has a new degree of freedom, *i.e.* the stacking chirality. For example, in TDBG, the AB-AB and AB-BA configurations have distinct stacking chirality arrangement, but very similar band structures [5–8]. Neither the isolated topological flat band nor the stacking chirality is present in the celebrated twisted bilayer graphene (TBG).

However, the total Chern number of the topological flat bands in TMG is always zero due to time reversal symmetry [6–8]. A possible improvement is via Floquet engineering using circularly polarized light (CPL), which can break time reversal symmetry and effectively produce non-equilibrium topological phases [27–36]. Intriguingly, several recent works illustrated that CPL irradiation can give rise to isolated Floquet flat bands with nonzero total Chern number in TBG [37–40], which offers an attractive platform to realize the so-called “Floquet fractional Chern insulator” [41]. It is natural to expect that CPL

may induce more complicated and interesting phenomena in TMG, due to its complex structure and novel topological properties. More interestingly, in valleytronics, CPL is a rather effective way to manipulate the valley degree of freedom in honeycomb lattices, such as bilayer graphene, MoS<sub>2</sub>, *etc* [42–50]. Thus, whether the CPL is able to give rise to some valley-related phenomena in TMG is also a worthwhile question, since the studies about how to manipulate the valley degree of freedom of moiré flat bands is still rare.

In this work, we study the CPL irradiation induced Floquet-Bloch band structures of the TMG systems. We show that, near the charge neutrality point, TMG always has two isolated Floquet Chern flat bands in the presence of CPL irradiation. Most importantly, we find that with the help of CPL irradiation, we can selectively split the valley degeneracy of TMG, and thus generate an optical controlled valley-polarized Floquet Chern flat band with tunable large Chern number. We reveal the Chern-number hierarchy rules of the Floquet flat bands in the (M+N)-layer TMG, which strongly relies on the stacking chirality of TMG. An intuitive explanation about why the TMG with different stacking chirality have distinct responses to CPL is also given. Since CPL is able to control the valley polarization of the Floquet flat bands in TMG, we expect that many of the valley-related properties of TMG [22], like orbital ferromagnetism, quantum anomalous hall effect, magneto-optical and nonlinear optical properties, can be switched by CPL. Our work thus opens up new opportunities to study the valleytronics of moiré flat bands.

*Models.*— We consider a (M+N)-layer TMG in the presence of CPL irradiation. In Figs. 1(a) and 1(b), we first illustrate the two distinct stacking chiralities of the

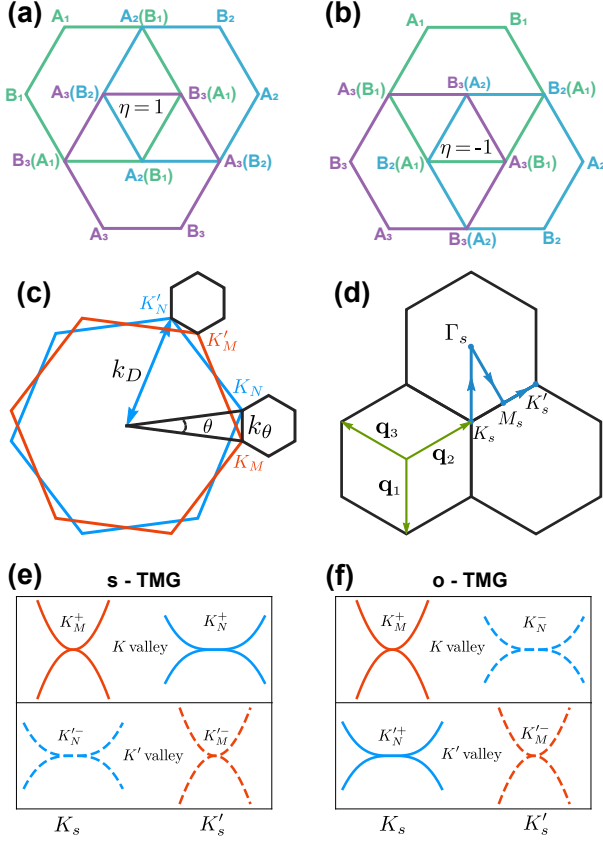


FIG. 1. (a) and (b) are respectively the schematics the chirally stacked MGs with  $\eta = \pm 1$  stacking chirality. Here,  $A_2$  means A site in layer 2, and so on. (c) Brillouin-zone (BZ) of the top (M-layer, red) and bottom (N-layer, blue) MGs. The black hexagon represent the moiré Brillouin-zone (mBZ) of TMG. (d) A larger version of mBZ. (e) and (f) illustrate the valley chirality of the MGs for each moiré valley. The case when two MGs have the same stacking chirality, like AB-AB TDBG, is given in (e); while (f) is for the opposite case, *e.g.* AB-BA TDBG.

ABC-stacked MG [51–53], where the ABC (CBA) configuration is denoted as  $\eta = 1$  ( $\eta = -1$ ). Here,  $\eta$  is the index of stacking chirality. Thus, TMG can be divided into two categories: s-TMG where two MGs have same stacking chirality (like AB-AB TDBG) and o-TMG with opposite stacking chirality (like AB-BA TDBG).

We consider the TMG with small twist angle  $\theta$  near the first magic angle [6–8, 54–56]. The corresponding moiré Brillouin zone (mBZ) (black lines) is given in Fig. 1 (c), where red (blue) line is the BZ of the top M-layer (bottom N-layer) MG. We see that the two MGs give a pair of  $K$  valley ( $K_M$  and  $K_N$ ) and a pair of  $K'$  valley ( $K'_M$  and  $K'_N$ ). Meanwhile, the moiré interlayer hybridization only mix the adjacent two valleys near either  $K$  or  $K'$ , while the interaction between distant valleys are tiny. Thus, valley is also a good quantum number of TMG, which are denoted as  $K$  ( $\tau = +1$ ) and  $K'$  ( $\tau = -1$ ) moiré

valley. Here,  $\tau$  is the moiré valley index.

A notable feature is the chirality of MG valleys, which will significantly influence the CPL effects as shown later. We know that the two inequivalent valleys in MG have opposite chirality, which also rely on its stacking chirality. Without loss of generality, we fix the stacking chirality of the top M-layer MG to be  $\eta = +1$  and define the chirality of its  $K$  valley as “+”, which is denoted as  $K_M^+$ . Then, for the s-TMG, the moiré valley  $K$  ( $K'$ ) is composed of  $K_M^+$  and  $K_N^+$  ( $K_M^-$  and  $K_N^-$ ), as shown in Fig. 1 (e). In contrast, moiré valley  $K$  ( $K'$ ) of the o-TMG corresponds to  $K_M^+$  and  $K_N^-$  ( $K_M^-$  and  $K_N^+$ ), see Fig. 1 (f).

We assume a normal incident CPL, which is described by a vector potential  $\mathbf{A}(t) = A_0(\cos \Omega t, \xi \sin \Omega t)$ . Here,  $\xi = -1$  ( $\xi = +1$ ) represents a left (right) CPL, and  $A_0$ ,  $\Omega$  are the amplitude and frequency, respectively. The time dependent Hamiltonian of the irradiated (M+N)-layer TMG in  $K$  valley is

$$H_{K,M+N}^{\eta,\eta'}(t) = \begin{pmatrix} H_{K,M}^{\eta}(t) & \mathbb{T} \\ \mathbb{T}^\dagger & H_{K,N}^{\eta'}(t) \end{pmatrix} + U, \quad (1)$$

where  $H_{K,M}^{\eta}(t)$  and  $H_{K,N}^{\eta'}(t)$  describe the top and bottom MGs, respectively.  $\mathbb{T}$  represents the moiré interlayer hopping, and  $U$  models the gate induced potential difference between layers. Specifically,

$$H_{K,M}^{\eta} = \begin{pmatrix} h_0(t) & h_{\eta} & 0 & \cdots \\ h_{\eta}^\dagger & h_0(t) & h_{\eta} & \cdots \\ 0 & h_{\eta}^\dagger & h_0(t) & \cdots \\ \vdots & \vdots & \vdots & \ddots \end{pmatrix}, \quad (2)$$

where  $h_0(t) = v_F \sigma \cdot [-i\hbar \nabla + eA(t)]$  is the Hamiltonian of monolayer graphene in  $K$  valley. The stacking chirality is reflected in the interlayer hopping matrix  $h_{\eta}$ , where  $h_{\eta=+} = \begin{pmatrix} 0 & 0 \\ t_{\perp} & 0 \end{pmatrix}$  and  $h_{\eta=-} = h_{\eta=+}^\dagger$  with  $t_{\perp}$  being the nearest neighbor interlayer hopping.  $\mathbb{T} = E_{M \times N} \otimes T(r)$ ,  $E_{M \times N}$  is a  $M \times N$  matrix with only one nonzero entry  $E_{M \times N}(M, 1) = 1$ .  $T(r) = \sum_{n=1}^3 T_n e^{-i\mathbf{q}_n \cdot \mathbf{r}}$  is the twist tunneling matrix of TMG, where  $\mathbf{q}_{n+1} = k_{\theta}(\sin n\phi, -\cos n\phi)$ ,  $\phi = 2\pi/3$ ,  $k_{\theta} = 2k_D \sin(\theta/2)$ , see in Figs. 1 (c) and (d).  $T_{n+1} = w_{AA}\sigma_0 + w_{AB}(\sigma_x \cos n\phi + \sigma_y \sin n\phi)$ , where  $w_{AA}$  ( $w_{AB}$ ) represents the tunneling amplitude of the intra- (inter-) sublattice.  $U = \text{diag}(M - \frac{1}{2}, \dots, \frac{1}{2}, -\frac{1}{2}, \dots, -N + \frac{1}{2}) \otimes \Delta_E \sigma_0$ , where  $\Delta_E$  is the gate induced potential difference between adjacent layers.

In high frequency limit, according to the Floquet band theory, a reasonable approximation is to expand the time dependent Hamiltonian in Eq. (1) to the first order of  $1/\Omega$  [32, 33],

$$H_{K,M+N}^{F,\eta,\eta'} = H_{K,M+N}^{(0),\eta,\eta'} + \Delta_{\Omega} I_{M+N} \otimes \sigma_z + U, \quad (3)$$

where  $H_{K,M+N}^{(0),\eta,\eta'}$  is the TMG Hamiltonian without irradiation. An important message is that the CPL give rise

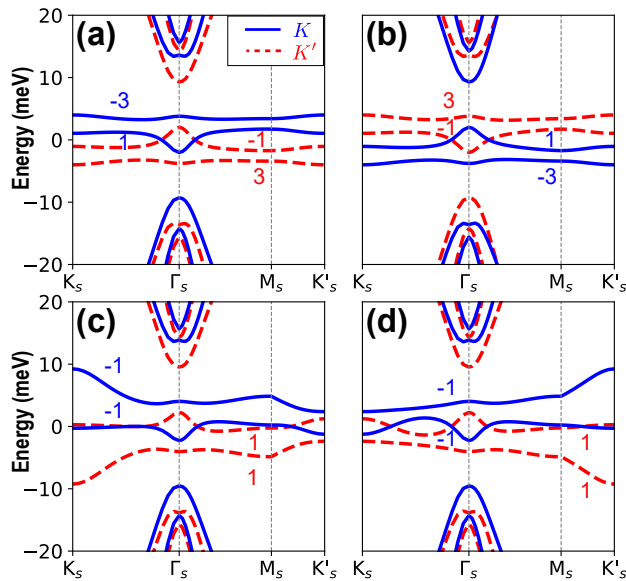


FIG. 2. Floquet band structures of the AB-BA TDBG at  $\theta = 1.05^\circ$ . (a) Left CPL with  $\Delta_\Omega = 4$  meV,  $\Delta_E = 0$  meV. (b) Right CPL with  $\Delta_\Omega = -4$  meV,  $\Delta_E = 0$  meV. (c) Left CPL with  $\Delta_\Omega = 4$  meV,  $\Delta_E = 3.5$  meV. (d) Left CPL with  $\Delta_\Omega = 4$  meV,  $\Delta_E = -3.5$  meV.

to an additional mass term in Eq. (3). Here,  $I_{M+N}$  is an identity matrix of order  $M+N$  and  $\Delta_\Omega = \xi(ev_F A_0)^2/\hbar\Omega$ .

The parameters for the MG used in this article is adapted from Ref. [7] and we record them here for convenience:  $t_0 \equiv 2\hbar v_F/\sqrt{3}a_0 = -3.1$  eV is the intra-layer nearest neighbour hopping with  $a_0 = 2.46$  Å and  $v_F \approx 1.0 \times 10^6$  m/s;  $w_{AB} = 0.12$  eV,  $w_{AA} = 0.098$  eV and  $t_\perp \approx 3w_{AB} = 0.36$  eV. For a 4 meV  $\Delta_\Omega$  with photon energy  $\hbar\Omega = 1.5$  eV [39], the electrical field strength of the CPL is about  $1.76 \times 10^3$  KV/cm and the intensity is about  $4.11 \times 10^9$  watt/cm<sup>2</sup>, which should be feasible in experiments with ultrafast laser technique [57, 58].

*Floquet Chern flat bands in TDBG.*—We take the TDBG as a paradigm to illustrate the CPL effects on TMG. We first discuss the case of AB-BA TDBG, as an example of o-TMG. The most remarkable result is that it has two separated and valley-split Floquet Chern flat bands with nonzero total Chern number. Figs. 2 (a) and 2 (b) show the Floquet band structures of AB-BA TDBG at  $\theta = 1.05^\circ$  around the first magic angle under left and right CPL, respectively. In each moiré valley, we have two nearly flat bands near the charge neutrality point, which are separated by a gap about 1.5 meV. Note that the gap is due to the applied CPL and can be increased with larger  $\Delta_\Omega$ , while in pristine TDBG the two flat bands are touched at the  $K_s$  and  $K'_s$  points [marked in Fig. 1(d)]. The energy of the two Floquet flat bands are valley-dependent. As shown in Fig. 2(a), with left CPL, the valence band in the moiré  $K'$  valley (red dashed lines) is lower than that in the  $K$  valley (blue solid lines).

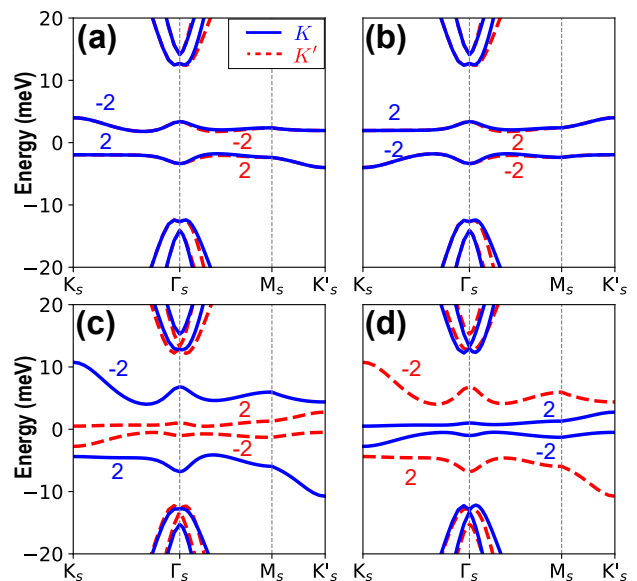


FIG. 3. Floquet band structures of the AB-AB TDBG at  $\theta = 1.05^\circ$ . (a) Left CPL with  $\Delta_\Omega = 4$  meV,  $\Delta_E = 0$  meV. (b) Right CPL with  $\Delta_\Omega = -4$  meV,  $\Delta_E = 0$  meV. (c) Left CPL with  $\Delta_\Omega = 4$  meV,  $\Delta_E = 4.5$  meV. (d) Left CPL with  $\Delta_\Omega = 4$  meV,  $\Delta_E = -4.5$  meV.

The case becomes opposite when a right CPL is applied, see Fig. 2 (b). It means that, in AB-BA TDBG, a valley-polarized flat band can be selectively generated by CPL with different polarization. Meanwhile, these flat bands are topologically nontrivial, for which the valley Chern number and the total Chern number are both nonzero. For example, in Fig. 2(a), the valley Chern numbers of the valence band in  $K$  and  $K'$  valleys are  $C_{Lv}^K = 1$  and  $C_{Lv}^{K'} = 3$ , respectively. Thus, the total Chern number of the valence band is  $C_{Lv}^{tot} = C_{Lv}^K + C_{Lv}^{K'} = 4$ . The nonzero total Chern number is allowed here since time reversal symmetry is broken by CPL. If the polarization of CPL is changed, the total Chern number changes sign, see Fig. 2(b). The topological properties of the flat bands can be further adjusted by a gate-induced perpendicular electric field represented by  $\Delta_E$ . In Figs. 2(c) and 2(d), with  $\Delta_E = \pm 3.5$  meV, the valley Chern numbers in both valleys change.

As shown in Fig. 1 (f), the moiré  $K$  ( $K'$ ) valley of o-TMG is formed by mixing two opposite chirality MG valleys  $K_M^+$  and  $K_N^-$  ( $K_M'^-$  and  $K_N'^+$ ). Specifically, the states at  $K_s$  point are mainly formed by electrons from the positive chirality MG valleys, while that at  $K'_s$  point are from negative chirality MG valleys. We know that, for irradiated MG, the CPL induced mass terms have opposite sign in the two valleys depending on their chirality, while the gate voltage induced one have the same sign [59, 60]. Hence, CPL induced mass term have opposite sign at  $K_s$  and  $K'_s$ , while that induced by electric field have the same sign. Consequently, due to the com-

petition between  $\Delta_\Omega$  and  $\Delta_E$ , when gradually increasing the gate voltage,  $\Delta_E > 0$  for example, the gap at  $K_s$  point enlarges, while the gap at  $K'_s$  point first diminishes and then reopens, resulting in the valley Chern numbers change in both moiré valley and the imbalanced gaps open at  $K_s$  and  $K'_s$  points.

Now, we turn to the case of AB-AB TDBG, *i.e.* an example of s-TMG. First, with only CPL, we cannot split the valley degeneracy. The Floquet bands of AB-AB TDBG under left and right CPL are shown in Figs. 3(a) and 3(b), respectively. With left (right) CPL, we get two separated Floquet flat bands with  $C_{Lc}^K = -2$ ,  $C_{Lv}^K = 2$  ( $C_{Rc}^K = 2$ ,  $C_{Rv}^K = -2$ ), *etc.* There are two obvious differences between the AB-AB and AB-BA cases. One is that the energy of flat bands in two moiré valleys are mixed in the AB-AB situation, and the other is that their corresponding valley Chern numbers are different. However, the total Chern number of the conduction or valance flat bands are the same, *e.g.*  $C_{Lv}^{tot} = 4$  as in Fig. 3(a) and Fig. 2(a).

Interestingly, the valley degeneracy in AB-AB TDBG can be further lifted by an additional vertical electric field. In Fig. 3(c), we apply a left CPL ( $\Delta_\Omega = 4$  meV) and a perpendicular electric field ( $\Delta_E = 4.5$  meV). The applied electric field induces a valley-dependent energy shift, and now the valence band in  $K$  valley is lower than that in  $K'$  valley. In contrast, when we reverse the direction of electric field, the valence band in the  $K'$  valley has lower energy, see in Fig. 3(d). So, in the AB-AB TDBG, we can also selectively get a valley-polarized Floquet Chern flat band via the combination effect of CPL and vertical electric field. The electric field can also change the valley Chern number, see in Figs. 3(c) and 3(d). For example, with large enough positive  $\Delta_E$  [Fig. 3(c)], the valley Chern numbers in  $K$  valley is invariant, while that of the  $K'$  valley is changed. Consequently, the total Chern number of each flat band becomes zero, which indicates a transition from quantum anomalous hall state to quantum valley hall state.

As shown in Fig. 1(e), for the s-TMG, the  $K$  moiré valley is formed by the  $K_M^+$  and  $K_N^+$  MG valleys, while  $K'$  moiré valley is formed by  $K_N^-$  and  $K_M^-$ . So, with similar reason as before, the mass term induced by CPL now will be opposite in sign for the two moiré valleys, and the electrical field induced one have the same sign at the two moiré valleys. When gradually increasing the gate voltage, the gap at one moiré valley further increases and the gap at the other first diminishes and then reopens, resulting in the moiré-valley-contrasting gap and the valley Chern number change only in one moiré valley. We see that the valley polarization mechanisms for o-TMG and s-TMG are different, and their different responses to CPL are caused by the interplay between the valley selective nature of CPL and the stacking chirality induced distinct MG valleys combination.

A valley-polarized flat band has many novel features, such as orbital ferromagnetism, magneto-optical effect, *etc* [22]. Now, we have demonstrated that the valley polarization in TMG can be selectively generated by Floquet engineering with CPL, so that many of these novel properties may be controlled by CPL irradiation. For example, we predict that CPL is able to generate and switch orbital ferromagnetism in TMG. Meanwhile, we anticipate that if superconductivity is formed, it may favor an exotic FFLO states [61, 62].

TABLE I. Valley Chern numbers of the (M+N)-layer TMG. The upper part is for s-TMG and lower part is for o-TMG.

M	N	$C_{Lc}^K$	$C_{Lv}^K$	$C_{Lc}^{K'}$	$C_{Lv}^{K'}$	$C_{Rc}^K$	$C_{Rv}^K$	$C_{Rc}^{K'}$	$C_{Rv}^{K'}$
2	2	-2	2	-2	2	2	-2	2	-2
2	3	-2	3	-3	2	3	-2	2	-3
3	3	-3	3	-3	3	3	-3	3	-3
2	4	-2	4	-4	2	4	-2	2	-4
M	N	-M	N	-N	M	N	-M	M	-N
2	2	-3	1	-1	3	1	-3	3	-1
2	3	-4	1	-1	4	1	-4	4	-1
3	3	-5	1	-1	5	1	-5	5	-1
2	4	-5	1	-1	5	1	-5	5	-1
M	N	-M-N+1	1	-1	M+N-1	1	-M-N+1	M+N-1	-1

*Floquet Chern flat bands of (M+N)-layer TMG.*—The main features of the Floquet flat bands in a general (M+N)-layer TMG are quite like that in TDBG, *i.e.* two separated Chern flat bands near the fermi level. It is because that all the ABC-stacked MGs have similar band structure. Most importantly, the CPL induced valley splitting is valid for all the TMGs. The main difference is the topological features of the Floquet flat bands. Here, we find a Chern number hierarchy rule of the Floquet flat bands in the (M+N)-layer TMG: (1) For s-TMG, the valley Chern number is

$$C_{\xi\zeta}^\tau = -\xi\zeta [M\Theta(\xi\tau\zeta) + N\Theta(-\xi\tau\zeta)], \quad (4)$$

where  $\Theta$  is the Heaviside function,  $\zeta$  is the band index for the conduction ( $\zeta = +1$ ) and valence ( $\zeta = -1$ ) band,  $\tau$  denotes the moiré valley and  $\xi$  represents the polarization of CPL as mentioned before. (2) For o-TMG,

$$C_{\xi\zeta}^\tau = -\xi\zeta [M\Theta(\xi\tau\zeta) + N\Theta(-\xi\tau\zeta)] - \tau(N - 1). \quad (5)$$

Equation (4) and (5) are summarized from our numerical results (see the Table I). Interestingly, the total Chern number of either conduction or valence band is  $-\xi\zeta(M + N)$ , which is irrelevant to the stacking chirality. Another rule of Chern number is about the total Chern number of the conduction and valence bands in each moiré valley. In s-TMG, the sum of valley Chern number in a single moiré valley equals  $-\tau(M - N)$ , while for the o-TMG, it is  $-\tau(M + N - 2)$ . This rule is irrelative with polarization of light, and origins from the fact that, within the parameter

regime used in this article, the two central flat bands are separated from other higher energy bands [8].

*Summary.*— In summary, we have studied the Floquet flat bands in the TMG systems. We illustrate that CPL can selectively produce a valley-polarized Floquet Chern flat band with tunable large Chern number. It offers a feasible way to manipulate the valley degree of freedom of the moiré flat bands, and thus opens new opportunities to study valleytronics in moiré flat band systems. We predict that many of the valley-related phenomena in TMG can be switched by CPL, *e.g.* optical controlled orbital ferromagnetism. We reveal that CPL effects here strongly rely on the stacking chirality of TMG, and we also find a Chern number hierarchy rule for the Floquet flat bands in TMG.

*Note added.* We note an independent theoretical work discussing the Floquet engineering in twisted double bilayer graphene [63].

Ming Lu thanks Hua Jiang, Robert Joynt and Jianpeng Liu for helpful discussions. This work is supported by the National Natural Science Foundation of China (Grants No. 11534001, 11874160, 11274129, 11874026, 61405067), and the Fundamental Research Funds for the Central Universities (HUST: 2017KFYXJJ027), and NBRPC (Grants No. 2015CB921102).

\* [jinhua@hust.edu.cn](mailto:jinhua@hust.edu.cn)

† [xcxie@pku.edu.cn](mailto:xcxie@pku.edu.cn)

- [1] Y. Cao, D. Rodan-Legrain, O. Rubies-Bigorda, J. M. Park, K. Watanabe, T. Taniguchi, and P. Jarillo-Herrero, *Nature* **583**, 215 (2020).
- [2] X. Liu, Z. Hao, E. Khalaf, J. Y. Lee, Y. Ronen, H. Yoo, D. Najafabadi, K. Watanabe, T. Taniguchi, A. Vishwanath, and P. Kim, *Nature* **583**, 221 (2020).
- [3] C. Shen, Y. Chu, Q.-S. Wu, N. Li, S. Wang, Y. Zhao, J. Tang, L. Jieying, J. Tian, K. Watanabe, T. Taniguchi, R. Yang, Z. Y. Meng, D.-X. Shi, O. Yazyev, and G. Zhang, *Nat. Phys* **16**, 1 (2020).
- [4] G. W. Burg, J. Zhu, T. Taniguchi, K. Watanabe, A. H. MacDonald, and E. Tutuc, *Phys. Rev. Lett.* **123**, 197702 (2019).
- [5] Y.-H. Zhang, D. Mao, Y. Cao, P. Jarillo-Herrero, and T. Senthil, *Phys. Rev. B* **99**, 075127 (2019).
- [6] M. Koshino, *Phys. Rev. B* **99**, 235406 (2019).
- [7] N. R. Chebrolu, B. L. Chittari, and J. Jung, *Phys. Rev. B* **99**, 235417 (2019).
- [8] J. Liu, Z. Ma, J. Gao, and X. Dai, *Phys. Rev. X* **9**, 031021 (2019).
- [9] Y. W. Choi and H. J. Choi, *Phys. Rev. B* **100**, 201402 (2019).
- [10] J. Y. Lee, E. Khalaf, S. Liu, X. Liu, Z. Hao, P. Kim, and A. Vishwanath, *Nat. Commun.* **10** (2019).
- [11] F. Wu and S. Das Sarma, *Phys. Rev. B* **101**, 155149 (2020).
- [12] G. Chen, A. L. Sharpe, P. Gallagher, I. T. Rosen, E. J. Fox, L. Jiang, B. Lyu, H. Li, K. Watanabe, T. Taniguchi, J. Jung, Z. Shi, D. Goldhaber-Gordon, Y. Zhang, and F. Wang, *Nature* **572**, 215 (2019).
- [13] G. Chen, L. Jiang, S. Wu, B. Lyu, H. Li, B. L. Chittari, K. Watanabe, T. Taniguchi, Z. Shi, J. Jung, Y. Zhang, and F. Wang, *Nat. Phys* **15**, 237 (2019).
- [14] B. L. Chittari, G. Chen, Y. Zhang, F. Wang, and J. Jung, *Phys. Rev. Lett.* **122**, 016401 (2019).
- [15] W.-J. Zuo, J.-B. Qiao, D.-L. Ma, L.-J. Yin, G. Sun, J.-Y. Zhang, L.-Y. Guan, and L. He, *Phys. Rev. B* **97**, 035440 (2018).
- [16] E. Suárez Morell, M. Pacheco, L. Chico, and L. Brey, *Phys. Rev. B* **87**, 125414 (2013).
- [17] Z. Ma, S. Li, Y.-W. Zheng, M.-M. Xiao, H. Jiang, J.-H. Gao, and X. C. Xie, [arXiv:1905.00622](https://arxiv.org/abs/1905.00622).
- [18] R. Bistritzer and A. H. MacDonald, *Proc. Natl. Acad. Sci. USA* **108**, 12233 (2011).
- [19] X. Li, F. Wu, and A. H. MacDonald, [arXiv:1907.12338](https://arxiv.org/abs/1907.12338).
- [20] S. Carr, C. Li, Z. Zhu, E. Kaxiras, S. Sachdev, and A. Kruchkov, *Nano Lett.* **20**, 3030 (2020).
- [21] Z. Ma, S. Li, M.-M. Xiao, Y.-W. Zheng, M. Lu, H. Liu, J.-H. Gao, and X. C. Xie, [arXiv:2001.07995](https://arxiv.org/abs/2001.07995).
- [22] J. Liu and X. Dai, *Npj Quantum Mater.* **6**, 57 (2020).
- [23] Y. Shi, S. Xu, M. M. Al Ezzi, N. Balakrishnan, A. Garcia-Ruiz, B. Tsim, C. Mullan, J. Barrier, N. Xin, B. A. Piot, T. Taniguchi, K. Watanabe, A. Carvalho, A. Mishchenko, A. K. Geim, V. I. Fal'ko, S. Adam, A. Helio Castro Neto, and K. S. Novoselov, [arXiv:2004.12414](https://arxiv.org/abs/2004.12414).
- [24] Y. Park, B. Lingam Chittari, and J. Jung, [arXiv:2005.01258](https://arxiv.org/abs/2005.01258).
- [25] H. Polshyn, J. Zhu, M. A. Kumar, Y. Zhang, F. Yang, C. L. Tschirhart, M. Serlin, K. Watanabe, T. Taniguchi, A. H. MacDonald, and A. F. Young, [arXiv:2004.11353](https://arxiv.org/abs/2004.11353).
- [26] S. Chen, M. He, Y.-H. Zhang, V. Hsieh, Z. Fei, K. Watanabe, T. Taniguchi, D. H. Cobden, X. Xu, C. R. Dean, and M. Yankowitz, [arXiv:2004.11340](https://arxiv.org/abs/2004.11340).
- [27] T. Oka and H. Aoki, *Phys. Rev. B* **79**, 081406 (2009).
- [28] T. Kitagawa, T. Oka, A. Brataas, L. Fu, and E. Demler, *Phys. Rev. B* **84**, 235108 (2011).
- [29] Z. Gu, H. A. Fertig, D. P. Arovas, and A. Auerbach, *Phys. Rev. Lett.* **107**, 216601 (2011).
- [30] Y. H. Wang, H. Steinberg, P. Jarillo-Herrero, and N. Gedik, *Science* **342**, 453 (2013).
- [31] G. Usaj, P. M. Perez-Piskunow, L. E. F. Foa Torres, and C. A. Balseiro, *Phys. Rev. B* **90**, 115423 (2014).
- [32] A. Eckardt and E. Anisimovas, *New J. Phys.* **17**, 093039 (2015).
- [33] T. Mikami, S. Kitamura, K. Yasuda, N. Tsuji, T. Oka, and H. Aoki, *Phys. Rev. B* **93**, 144307 (2016).
- [34] C.-K. Chan, P. A. Lee, K. S. Burch, J. H. Han, and Y. Ran, *Phys. Rev. Lett.* **116**, 026805 (2016).
- [35] X.-X. Zhang, T. T. Ong, and N. Nagaosa, *Phys. Rev. B* **94**, 235137 (2016).
- [36] T. Oka and S. Kitamura, *Annu. Rev. Condens. Matter Phys.* **10**, 387 (2019).
- [37] G. E. Topp, G. Jotzu, J. W. McIver, L. Xian, A. Rubio, and M. A. Sentef, *Phys. Rev. Research* **1**, 023031 (2019).
- [38] Y. Li, H. A. Fertig, and B. Seradjeh, [arXiv:1910.04711](https://arxiv.org/abs/1910.04711).
- [39] O. Katz, G. Refael, and N. H. Lindner, [arXiv:1910.13510](https://arxiv.org/abs/1910.13510).
- [40] M. Vogl, M. Rodriguez-Vega, and G. A. Fiete, *Phys. Rev. B* **101**, 235411 (2020).
- [41] A. G. Grushin, A. Gómez-León, and T. Neupert, *Phys. Rev. Lett.* **112**, 156801 (2014).
- [42] D. Xiao, W. Yao, and Q. Niu, *Phys. Rev. Lett.* **99**, 236809 (2007).

- [43] D. S. L. Abergel and T. Chakraborty, *Appl. Phys. Lett.* **95**, 062107 (2009).
- [44] D. Abergel and T. Chakraborty, *Nanotechnology* **22**, 015203 (2011).
- [45] T. Cao, G. Wang, W. Han, H. Ye, C. Zhu, J. Shi, Q. Niu, P. H. Tan, E. Wang, B. Liu, and J. Feng, *Nat. Commun.* **3**, 887 (2012).
- [46] D. Xiao, G.-B. Liu, W. Feng, X. Xu, and W. Yao, *Phys. Rev. Lett.* **108**, 196802 (2012).
- [47] X. Zhai and G. Jin, *Phys. Rev. B* **89**, 235416 (2014).
- [48] J. Schaibley, H. Yu, G. Clark, P. Rivera, J. Ross, K. Seyler, W. Yao, and X. Xu, *Nat. Rev. Mater* **1**, 16055 (2016).
- [49] A. Kundu, H. A. Fertig, and B. Seradjeh, *Phys. Rev. Lett.* **116**, 016802 (2016).
- [50] E. Sie, C. H. Lui, Y.-H. Lee, L. Fu, J. Kong, and N. Gedik, *Science* **355**, 1066 (2017).
- [51] H. Min and A. H. MacDonald, *Phys. Rev. B* **77**, 155416 (2008).
- [52] F. Zhang, B. Sahu, H. Min, and A. H. MacDonald, *Phys. Rev. B* **82**, 035409 (2010).
- [53] J. Jung, F. Zhang, Z. Qiao, and A. H. MacDonald, *Phys. Rev. B* **84**, 075418 (2011).
- [54] J. M. B. Lopes dos Santos, N. M. R. Peres, and A. H. Castro Neto, *Phys. Rev. Lett.* **99**, 256802 (2007).
- [55] J. M. B. Lopes dos Santos, N. M. R. Peres, and A. H. Castro Neto, *Phys. Rev. B* **86**, 155449 (2012).
- [56] R. Bistritzer and A. H. MacDonald, *Proc. Natl. Acad. Sci.* **108**, 12233 (2011).
- [57] G. A. Mourou, C. P. J. Barry, and M. D. Perry, *Phys. Today* **51**, 22 (1998).
- [58] J. W. McIver, B. Schulte, F.-U. Stein, T. Matsuyama, G. Jotzu, G. Meier, and A. Cavalleri, *Nat. Phys* **16**, 38 (2019).
- [59] C. Qu, C. Zhang, and F. Zhang, *2D Materials* **5**, 011005 (2017).
- [60] S. Li, C.-C. Liu, and Y. Yao, *New J. Phys.* **20**, 033025 (2018).
- [61] P. Fulde and R. A. Ferrell, *Phys. Rev.* **135**, A550 (1964).
- [62] A. I. Larkin and Y. N. Ovchinnikov, *Zh. Eksp. Teor. Fiz.* 47,1136(1964).
- [63] M. Rodriguez-Vega, M. Vogl, and G. A. Fiete, [arXiv:2006.04297](https://arxiv.org/abs/2006.04297).